The Department of Electrical and Electronic Engineering
University of Auckland
New Zealand

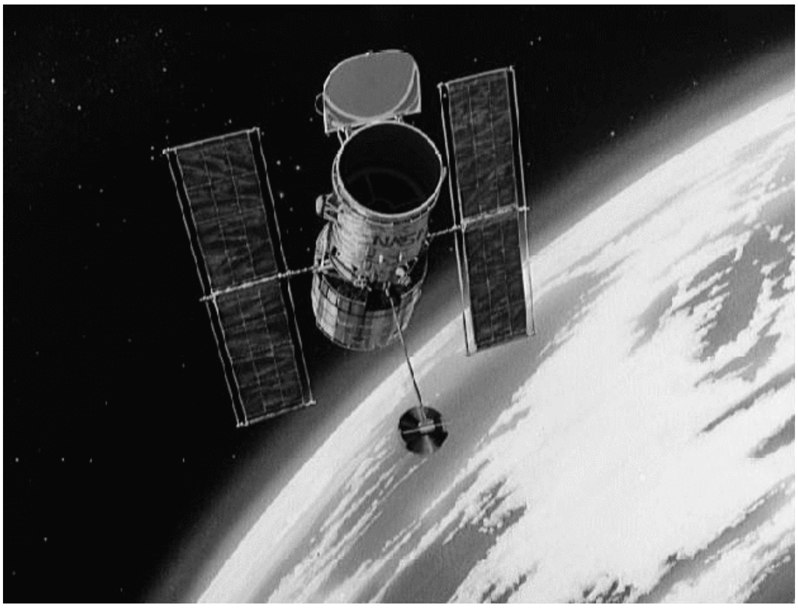

Accelerated Iterative Blind Deconvolution

David S. C. Biggs

December 1998

The University of Auckland

A THESIS SUBMITTED IN PARTIAL FULFILLMENT
OF THE REQUIREMENTS FOR THE DEGREE OF
DOCTOR OF PHILOSOPHY IN ENGINEERING

Abstract

This thesis considers the problem of restoring an image distorted by a linear spatially-invariant point spread function (PSF) and corrupted by noise. A principle aim is to develop techniques that are practical and require a minimum amount of prior knowledge. The process of deconvolution is attempted using least-squares and maximum-likelihood iterative algorithms. A survey of the literature introduces the main techniques for deconvolution when the PSF is known, and various approaches for achieving blind deconvolution—estimating both the PSF and the underlying object from the blurred observation. The two main areas of focus for this thesis are accelerating iterative image restoration algorithms, and developing blind deconvolution methods for extended objects.

The first main contribution is the development of an acceleration technique to speed the rate of convergence of iterative algorithms that use successive approximation. The acceleration uses a vector extrapolation approach which eliminates the need to compute the gradient of an objective function, or to perform a line search optimisation. The performance is comparable to that of conjugate gradient optimisation, and an example maximum-entropy restoration reduces the number of iterations from 1,000 to 27. A simple modification to the extrapolation allows the acceleration of the Richardson-Lucy (RL) iteration while implicitly imposing the positivity constraint.

The second contribution is the development of blind deconvolution algorithms that do not require spatial or spectral constraints to produce a solution, and can be used on extended objects. The key to achieving this is to recognise that the image and PSF estimates may required different amounts of restoration. By appropriately weighting the update of the image or PSF estimate a suitable result can be produced. Methods for achieving this using both joint- and alternating-variable optimisation are discussed. Issues regarding scaling of the variables are also addressed.

An iterative blind deconvolution method employing the RL algorithm, vector extrapolation, and different numbers of image and PSF iterations, is used to restore a variety of simulated and real images from terrestrial telescopes, the Hubble Space Telescope, multiframe speckle imaging, 3D wide-field fluorescence and confocal microscopes, and scanning electron microscopes. Methods for coping with Poisson noise corruption, and image boundary artifacts are also discussed.

Acknowledgments

Throughout the course of my PhD study I have benefited enormously from the assistance and support of many people to whom I am indebted.

My sincerest thanks to my supervisor, Dr Mark Andrews, who provided invaluable guidance and support throughout all stages of the PhD research and thesis development, and was always available to discuss the research (and many other topics).

I am grateful to Dr Richard Lane (University of Canterbury) for many informative discussions about deconvolution. Thanks also to Dr Ramakrishna Kakarala, Dr Andy Philpott (Engineering Science) and Professor Michael Saunders (Stanford University) for their suggestions and advice about several of the mathematical derivations.

I would also like to thank the following people and organisations:

Professor John Boys – who first proposed the project which has developed into this thesis.

Dr Jim Metson (Chemistry) – for the guidance provided during the initial stages of the research and funding for the equipment to capture images from the electron microscope.

David Stringer (Chemical and Materials) and Catherine Hobbis (Chemistry) – for their assistance in setting up the imaging system and capturing data from the instrument.

Dayl Brack, Evans Leung and Peter Barnes – who provided the technical and computing support.

Professor Robert Plemmons (Wake Forest University) – for the satellite data provided and for the invitation to the SPIE conference in 1998.

Russell Smith – for his assistance with many aspects of the thesis including the proof reading, and for his friendship.

All my friends who have made my time in the lab an enjoyable experience.

University of Auckland – for the award of a Doctoral Scholarship during the first three years of study, and conference travel funds through the Graduate Research Fund.

Royal Society of New Zealand – for the award of the 1995 RHT Bates Scholarship.

NASA JSC Digital Image Collection – where the artist concept of the Hubble Space Telescope used on the title page was obtained from (Photo ID: S90-34002).

Finally I owe the greatest debt of gratitude to my parents whose support and encouragement enabled me to focus on my research which resulted in this thesis becoming a reality.

Contents

List of symbols

The following lists the main symbols, operators and abbreviations used throughout the thesis. All equations and symbols are in italics, with matrices and vectors in boldface capitals and lowercase respectively. A two-dimensional image stored in an array can be converted into a vector by lexicographically ordering the elements. Symbols and abbreviations are defined the first time each appears. Capital letters represent the Fourier transforms of their lower case counterparts.

Mathematical variables

$\mathbf{f}$	Original undistorted image
$\mathbf{g}$	Degraded image
$\mathbf{n}$	Noise corruption
$\mathbf{H}$	Point spread function of the system
$\hat{\mathbf{f}}$	Estimate of original image
$\hat{\mathbf{f}}_k$	Estimate of original image after k iterations
$\mathbf{r}_k$	Reblurred image after k iterations ($\mathbf{H}\hat{\mathbf{f}}_k$)
$\mathbf{p}_k$	Gradient vector
$\mathbf{q}_k$	Search direction vector
$f(x, y)$	Original two-dimensional sampled image
$g(x, y)$	Sampled degraded image
$n(x, y)$	Corrupting noise at sampled points
$h(x, y)$	Sampled point spread function
$\hat{f}(x, y)$	Estimate of original image
$\hat{f}_k(x, y)$	Estimate of original image after k iterations
$\hat{h}(x, y)$	Estimate of original point spread function
$\hat{h}_k(x, y)$	Estimate of original point spread function after k iterations
$r_k(x, y)$	Reblurred image after k iterations
$w(x, y)$	Window function
$F(u, v)$	Discrete Fourier transform of $f(x, y)$
$G(u, v)$	Discrete Fourier transform of $g(x, y)$
$N(u, v)$	Discrete Fourier transform of $n(x, y)$
$H(u, v)$	Discrete Fourier transform of $h(x, y)$
$m \times n$	Image of size m by n pixels

$e(\cdot)$	Error function
σ	Standard deviation
$\mathbf{\Lambda_A}$	Eigenvalues of $\mathbf{A}$
$\mathbf{S}$	Eigenvectors
$\mathcal{L}$	Likelihood measure

Mathematical operators

$\sum$	Sum over all elements
$\prod$	Product of all elements
$\mathcal{F}[\cdot]$	Fourier transform
$\mathcal{F}^{-1}[\cdot]$	Inverse Fourier transform
$\lvert \cdot \rvert$	Absolute value
$\lVert \cdot \rVert^2$	L2-Norm (energy)
$\mathbf{H}^T$	Transpose of matrix $\mathbf{H}$
$\mathbf{H}^{-1}$	Inverse of matrix $\mathbf{H}$
$\mathbf{H}^P$	Pseudo inverse of matrix $\mathbf{H}$
$\otimes$	Convolution operator
$\star$	Correlation operator
$\odot$	Hadamard product
$\cdot$	Elementwise multiplication
$\log(\cdot)$	Natural logarithm
$\arg_x$	Argument x
max	Maximum
min	Minimum
$\triangleq$	Defined as being equal to
$p(\cdot)$	Probability
$\mathbf{z}^{-1}$	Single step digital delay

Abbreviations

2D	Two-Dimensional
3D	Three-Dimensional
AES	Auger Electron Spectrometer
AO	Adaptive Optics
AR	Autoregressive
ARMA	Autoregressive Moving Average
AVE	Additive Vector Extrapolation
BCCB	Block Circulant with Circulant Blocks
BF	Brightfield
CAT	Computed Axial Tomography
CCD	Charge Coupled Device
CG	Conjugate Gradient

CLS	Constrained Least-Squares
CLSM	Confocal Laser Scanning Microscope
COSTAR	Corrective Optics Space Telescope Axial Replacement
DOF	Degrees Of Freedom
EM	Expectation-Maximisation
ESO	European Southern Observatory
EVE	Exponential Vector Extrapolation
FBP	Filtered Back-Projection
FPB	Fractal Pixon Basis
FFT	Fast Fourier Transform
FR	Fletcher-Reeves
GCD	Grouped-variable Coordinate Descent
GCV	Generalised Cross Validation
GD	Gradient Descent
GOF	Goodness Of Fit
GS	Gerchberg-Saxton
HS	Hestenes-Stiefel
HST	Hubble Space Telescope
IBD	Iterative Blind Deconvolution
ICLS	Iterative Constrained Least-Squares
ICTM	Iterative Constrained Tikhonov-Miller
IDAC	Iterative Deconvolution Algorithm in C
IEEE	Institute of Electrical and Electronic Engineers
IMSE	Improved Mean Square Error
IPENZ	Institute of Professional Engineers of New Zealand
JPL	Jet Propulsion Laboratory
JSC	Johnson Space Center
LS	Least-Squares
MA	Moving Average
MAP	Maximum *a priori*
ME	Maximum Entropy
ML	Maximum-Likelihood
MMSE	Minimum Mean Square Error
MPE	Minimal Polynomial Extrapolation
MSE	Mean Square Error
NAS-RIF	Non-negativity And Support-constraints Recursive Inverse Filter
NGC	New General Catalogue (of nebulae and clusters of stars)
NGST	Next Generation Space Telescope
NICMOS	Near Infra-Red Camera and Multi-Object Spectrometer
NSR-RIF	Non-negativity and Support Regularised Recursive Inverse Filter
ODE	Ordinary Differential Equation
OSM	Optical Sectioning Microscopy
PC	Personal Computer
PET	Positron Emission Tomography
POCS	Projections Onto Convex Sets
PR	Polak-Ribière
PSF	Point Spread Function

RCSMS	Research Center for Surface and Materials Science
r.h.s.	Right Hand Side
RGB	Red, Green, Blue
RL	Richardson-Lucy
RRE	Reduced Rank Extrapolation
SAA	Shift-And-Added
SBIG	Santa Barbara Instrument Group
SD	Steepest Descent
SEM	Scanning Electron Microscopy
SNR	Signal-to-Noise Ratio
SOR	Successive Over-Relaxation
STSDAS	Space Telescope Science Data Analysis System
TIM	Telescope Image Modelling
TM	Tikhonov-Miller
UA	Unaccelerated
UPB	Uniform Pixon Basis
VE	Vector Extrapolation
WFF	Wide-Field Fluorescence
WFPC	Wide Field Planetary Camera